

The Role of the Cation in the Solvation of Cellulose by Imidazolium-Based Ionic Liquids

Brooks D. Rabideau,^{*,‡} Animesh Agarwal,^{†,§} and Ahmed E. Ismail^{*,‡}

[†]Aachener Verfahrenstechnik: Molecular Simulations and Transformations, Faculty of Mechanical Engineering, RWTH Aachen University, Schinkelstraße 2, 52062 Aachen, Germany

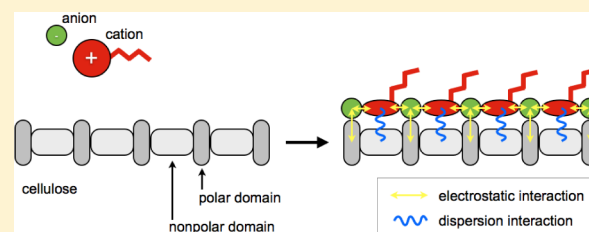
[‡]AICES Graduate School, RWTH Aachen University, Schinkelstraße 2, 52062 Aachen, Germany

[§]Institut für Mathematik, Freie Universität Berlin, Arnimallee 6, 14195 Berlin, Germany

Supporting Information

ABSTRACT: We present a systematic molecular dynamics study examining the roles of the individual ions of different alkyimidazolium-based ionic liquids in the solvation of cellulose. We examine combinations of chloride, acetate, and dimethylphosphate anions paired with cations of increasing tail length to elucidate the precise role of the cation in solvating cellulose. In all cases we find that the cation interacts with the nonpolar domains of cellulose through dispersion interactions, while interacting electrostatically with the anions bound at the polar domains of cellulose.

Furthermore, the structure and dimensions of the imidazolium head facilitate the formation of large chains and networks of alternating cations and anions that form a patchwork, satisfying both the polar and nonpolar domains of cellulose. A subtle implication of increasing tail length is the dilution of the anion concentration in the bulk and at the cellulose surface. We show how this decreased concentration of anions in the bulk affects hydrogen bond formation with cellulose and how rearrangements from single hydrogen bonds to multiple shared hydrogen bonds can moderate the loss in overall hydrogen bond numbers. Additionally, for the tail lengths examined in this study we observe only a very minor effect of tail length on the solvation structure and overall interaction energies.



INTRODUCTION

Despite production of over a trillion metric tons each year¹ and the allure of being a renewable, environmentally friendly feedstock, cellulose remains vastly underutilized in the production of both energy and high-value chemicals. In large part, this underutilization can be attributed to cellulose's strong resistance to dissolution, commonly referred to as recalcitrance.² While water and many common organic solvents have difficulty dissolving cellulose, a number of interesting solvent classes have been identified that are able to dissolve cellulose.³ These include certain amine oxides, mixtures of organic liquids and inorganic salts, aqueous bases, and, more recently, ionic liquids (ILs).^{4,5} ILs offer a number of distinct advantages over traditional solvents, including low volatilities⁶ and the ability to be tailored to meet specific physicochemical goals. Different cation–anion combinations and small changes in the structure of the individual ions can significantly impact the properties of an IL and its behavior in solution. Thus, there is great interest in trying to understand how the choice of specific ions and these different combinations affects not only dissolution^{5,7–11} but also other variables including cost, environmental impact, continued effectiveness in the presence of water^{12,13} or other impurities,¹⁴ and their ability to be recovered and recycled.¹⁵

The general consensus posits that a strong hydrogen-bond-accepting anion is critical for an IL's capacity to dissolve cellulose.^{10,16–18} NMR experiments and molecular dynamics

(MD) simulations have both shown that the predominant interaction between ILs and glucose appear to be hydrogen bonding between the anions and the sugar's hydroxyl groups.^{19,20} MD studies of the initial breakup of small crystalline bundles have already shown that anions bind to the external hydroxyl groups of cellulose and that the cations provide the bulk in separating these negatively charged moieties.²¹ Others, looking directly at the effect of cation structure, found that the presence of electron-withdrawing groups in the alkyl tail could enhance cations' interactions with cellulose.²² Though many view the cation as a supportive spectator in dissolution, several studies have suggested that the cation plays a more active role. Based upon NMR experiments, it has been argued that both the anions and the cations of [C₂mim]Ac form hydrogen bonds with cellulose,²³ although other researchers have voiced their skepticism of this interpretation.²⁴

The most notable example of the cation being the deciding factor in dissolution is a peculiar “odd–even effect” observed in alkyimidazolium chlorides.^{7,9} This study showed that cations with even tail lengths ($n = 2, 4$, or 6) dissolve cellulose, while cations with odd tail lengths ($n = 3, 5$) do not. Furthermore,

Received: November 25, 2013

Revised: January 19, 2014

Published: January 21, 2014

this strongly implied connection between the molecular structure of the ILs and their function motivates the use of MD simulations for the present study, probing length and time scales that remain inaccessible by experiments. Undoubtedly, there is to date neither clear consensus surrounding the precise role of the cation in dissolution nor an indication of the underlying cause of this peculiar “odd–even” behavior. A further understanding of the precise role of the cation in solvating cellulose could lead to ILs with improved performance or ultimately to even more cost-effective replacements.

In this paper we examine ILs composed of 1-alkyl-3-methylimidazolium cations, paired with chloride (Cl), acetate (Ac), and dimethylphosphate (DMP) anions. These ILs were selected because a number of them have shown the ability to dissolve cellulose with the added benefit of commercial availability. We examine the interaction and behavior of these ILs with an individual strand of cellulose using MD simulations. In the next section we provide a brief overview of the details of our simulations and the postprocessing methods used to quantify the metrics used in the analyses. We then explore the nature of the first solvation shell, finding that its structure is strongly determined by the interactions of anions with the hydroxyl groups of cellulose. We classify the different types of hydrogen bonds formed between the anions and cellulose and the effects of tail length and reduced anion concentration on these quantities. Next, we investigate the role of the cations in the solvation structure and answer the question of whether the cations interact with cellulose directly or with the anions bound at the cellulose surface. Finally, we calculate the interaction energies arising from the different ionic species and provide a complete picture of how the solvation structure equates with the favorable interaction energies with amphiphilic cellulose.

METHODS

Simulation Details. We studied a set of 15 different imidazolium-based ILs. We generically denote the structure of an IL as $[C_n\text{mim}]X$, where n is the length of the alkyl tail (see Figure 1) and X represents the anion (here, $X = \text{Cl}, \text{Ac}, \text{or}$

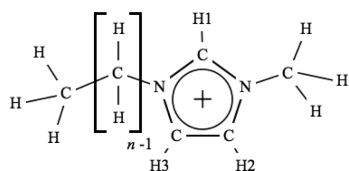


Figure 1. Chemical structure of the imidazolium-based cation.

DMP). For each anion, we studied the cases $n \in \{1, 2, 3, 4, 5\}$. These cases were specifically chosen for the present study because the “odd–even effect” is the most prominent at these short lengths.^{7,9} The imidazolium ions (see Figure 1) and chloride ions were modeled using the force field developed by Canongia Lopes,^{25,26} with all cationic C–H bonds held fixed using the SHAKE algorithm.²⁷ Acetate and dimethylphosphate were modeled using the OPLS-AA²⁸ force field. For cellulose (see Figure 2), we used the OPLS-2005 force field,^{28,29} which has been used in previous studies of cellulose dynamics.^{30,31} In the past, to accelerate aqueous simulations, the lengths of the O–H bonds in cellulose have been fixed and the time step increased to 2 fs.^{31,32} We found, however, that this was incompatible with the IL solvents. Therefore, we did not constrain the bonds and used a time step of 1 fs in all of our

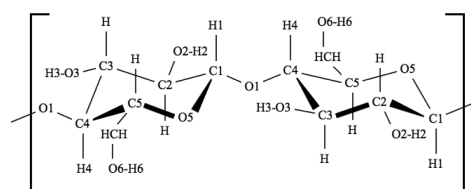


Figure 2. Chemical structure of the repeat biose unit of cellulose.

simulations. For further details on the naming of individual atoms within each structure please see Figure S1 of the Supporting Information.

Following *NPT* equilibration of each of the solvents for 3 ns in a $60 \text{ \AA} \times 60 \text{ \AA} \times 100 \text{ \AA}$ cell, a single strand of cellulose consisting of 16 glucose units was placed in each IL. The initial elongated state of the cellulose strand was taken from the crystallography data for the cellulose $I\beta$ state.³³ Cations and anions were removed in a 1:1 ratio to ensure sufficient space to accommodate the cellulose strand as well as maintain net charge neutrality. The resulting systems were then simulated for another 3 ns in an *NPT* ensemble at 400 K and 1 bar and continued for another 40 ns in the *NVT* ensemble at the same temperature.

Both ensembles were connected to a Nosé–Hoover thermostat with a thermocouple of 100 fs and the *NPT* ensemble contained an additional Nosé–Hoover barostat with a barocouple of 1000 fs. A cutoff of 12 Å was used for both the electrostatic and dispersion terms and long-range electrostatics computed with the particle–particle particle–mesh (PPPM) technique developed by Hockney and Eastwood³⁴ with an accuracy of 1 part in 10^4 . All MD simulations were performed with LAMMPS,³⁵ with atomic positions collected at 20 ps intervals. This frequency was used for all analyses discussed herein.

Additional simulations were also performed to determine whether the length of cellulose or the presence of additional chains would affect the quantities presented in this study. Simulations of a single chain consisting of 8, 16, or 32 glucans in $[C_2\text{MIM}]\text{Ac}$ as well as a simulation consisting of 4 strands of cellulose with 16 glucans per strand in $[C_2\text{MIM}]\text{Ac}$ were performed. These results can be found in Tables S1–S5 and Figure S2 of the Supporting Information. There were no significant differences between the 16 glucan strand and either the 32 glucan or the 4 strand cases, while there were just a few minor differences compared to the 8 glucan case. Thus, we consider the results for each of the 16 glucan strands presented in this paper to be representative of a cellulose chain of intermediate length.

Quantification of Contact, Solvation Structure, and Anion Bridging. To help determine if the anions and cations in an IL are in close proximity to the cellulose surface, we calculated the number of each species that could be considered “in contact” with a glucan. We define contact to be the presence of any atom of a given cation or anion within 3.5 Å of any cellulose atom. Through visual inspection this criteria appeared to be a strong indicator of the ions within the first solvation shell, as this distance is usually less than the average nearest-neighbor distance of the ILs.¹²

Associated with the concept of contact between an IL and cellulose, and between strands of cellulose, is the formation of hydrogen bonds. In MD simulations, hydrogen bonds are normally computed using geometric criteria.^{36–41} These criteria require that the distance between the two oxygens be less than

3.5 Å, the distance from the hydrogen to the oxygen acceptor be less than 2.45 Å, and the acceptor–donor–hydrogen angle be less than 30°. Similar to previous studies,²⁰ we distinguish here two main ways an ion can form hydrogen bonds with cellulose: bridging and nonbridging. A *bridging* arrangement allows a single ion to interact with two different hydrogens, either within a single glucan unit or between neighboring glucan units; if an anion interacts with just a single hydrogen, it is said to be *nonbridging*. Examples of nonbridging and bridging arrangements are shown in Figure 3.

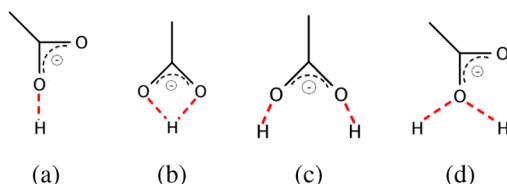


Figure 3. Examples of (a, b) nonbridging and (c, d) bridging acetate ions.

Additionally, we have computed spatial distribution functions (SDFs) of the positions of the various cations and anions relative to the cellulose molecule. In principle, the calculations proceed in much the same way as the calculation of radial distribution functions, except for being distributed in three-dimensional space rather than being a function only of the distance between particles. For a given system, we generally show isosurfaces which represent the region of space in which the concentration of a given type of particle is some multiple of the concentration expected for an isotropic distribution of particles (usually 3 or 5 times greater).

RESULTS AND DISCUSSION

Number of Ions in First Solvation Shell. A consequence of longer cation tail lengths is that the additional CH₂ groups effectively dilute the concentration of anions in the bulk. Figure 4a contains Cl–Cl radial distribution functions with increasing tail length for a simulation with neat IL (no cellulose) and demonstrates this dilution effect through increased Cl–Cl spacing as the tail lengths. This is also true of the acetates and to a much lesser extent the dimethylphosphate ions (see

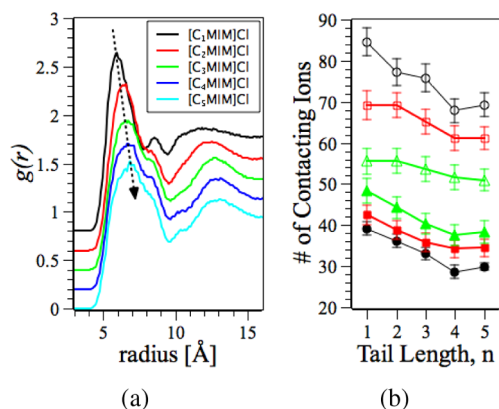


Figure 4. (a) Cl–Cl RDFs of the pure ILs. (b) Number of anions (filled symbols) and cations (open symbols) in the first solvation shell of the cellulose strand. Colors indicate (black ○) [C₁mim]Cl, (red □) [C_nmim]Ac, and (green △) [C_nmim]DMP. Vertical bars indicate the standard deviation.

Figure S3 of the Supporting Information). By measuring the number of ions in contact with the surface, we can examine if the changes occurring within the bulk are in fact reflected at the cellulose surface. The average numbers of contacting ions were calculated for the entire trajectory and are provided in Figure 4b.

The number of anions in contact with cellulose decreases as the tail length increases for each anion, reflecting the decreased anion concentration in the bulk. For the chlorides the number of anions per glucan drops by roughly 25%, from about 2.5 per glucan for [C₁mim]Cl to about 1.9 per glucan for [C₄mim]Cl and [C₅mim]Cl. Moreover, the number of contacting cations also decreases for all ILs, in conjunction with the increased molar volume of each cation as tail length increases. The differences seen in the cation–anion ratios at the surface appear proportional to differences in the ratios of the molecular volumes.

The Anion. Solvent Structure and Hydrogen Bonding. In the following sections we take a deeper look at the formation of anion–cellulose hydrogen bonds and the solvation structure to begin forming a more physical picture of the overall solvation behavior.

Spatial distribution functions (SDFs) were constructed around an individual glucan of cellulose, revealing the preferred locations of individual atoms within each of the ILs. In practice, the two terminal glucans were not considered and the 14 inner glucans were averaged together. The different anions showed many common characteristics, although a few distinct differences were also present. All three anions exhibit the behavior described below. However, because it is substantially easier to visualize and describe the behavior of chlorides, we focus on them here. It should be remembered, however, that this discussion also extends to both the acetates and the dimethylphosphates.

The locations of the chlorides around a representative glucan unit are displayed in Figure 5a. The green regions represent a superposition of all of the preferred locations of the chloride anions around cellulose. Because of the polymeric nature and stereochemical structure of cellulose, with each unit rotated

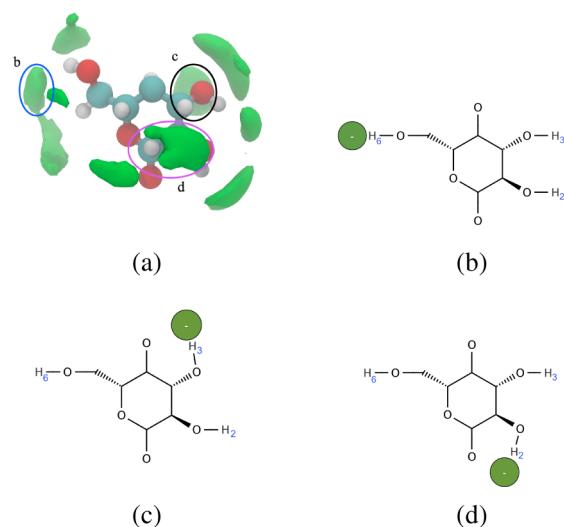


Figure 5. (a) Spatial distribution function showing the location of chlorides in [C₁mim]Cl around an individual glucan. Isosurfaces indicate 5 times the normal density. The labeled regions correspond with nonbridging anions at the (b) H₆ (c) H₃ and (d) H₂ sites.

180° axially from the previous unit, these preferred locations form a spiral along the long axis of cellulose. It should be kept in mind that the true IL structure at the cellulose surface is continually in flux during simulations. While anions form hydrogen bonds with specific hydroxyl groups and can persist for several nanoseconds, hydrogen bonds between different functional groups are continuously being formed and broken. Through visual inspection it is possible to determine which subregions corresponds to specific binding patterns of the anions with cellulose.

Three such nonbridging binding patterns are given in Figure 5 and represent the nonbridging anions near cellulose. Though a large proportion of these are observed at each time step and tend to be present in higher numbers at low tail lengths, a significant proportion of anion bridges are also present. Anion bridges with two or more hydroxyl groups tend to be longer-lived as a result of this binding redundancy. These bridging patterns, and their respective locations in the SDF, are given in Figure 6. As shown in this figure, these bridges can form

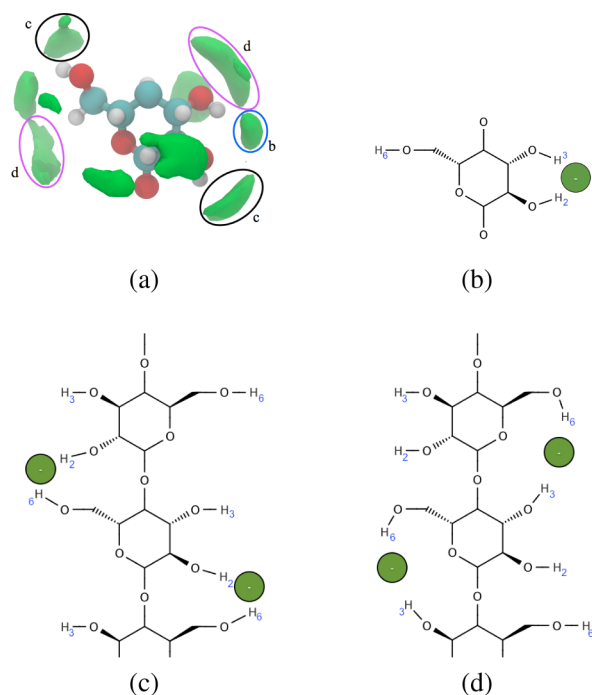


Figure 6. (a) Spatial distribution function showing the location of chlorides in [C₁mim]Cl around an individual glucan. Isosurfaces indicate 5 times the normal density. The labeled regions correspond with bridging (b) H_{2i}–H_{3i} (same glucan), (c) H_{2i}–H_{6j} (different glucan), and (d) H_{3i}–H_{6j} (different glucan) hydrogen bonds.

between two hydroxyl groups within the same glucan (Figure 6b noted as H_i–H_j, with *i* and *j* indicating the index of the glucan), or they can form between two hydroxyl groups belonging to two different glucans (Figure 6c,d), noted as H_i–H_j with *i* ≠ *j*).

The primary difference between the binding patterns shown above for the chlorides and that of the acetates and the dimethylphosphates was the increased prevalence of another major binding arrangement. The SDFs in these cases are so distinct that they reveal the preferred orientations in addition to just the locations of the anions relative to cellulose (Figure 7a,b). Figure 7c depicts the corresponding bridging pattern while Figure 7d shows an example produced during the run,

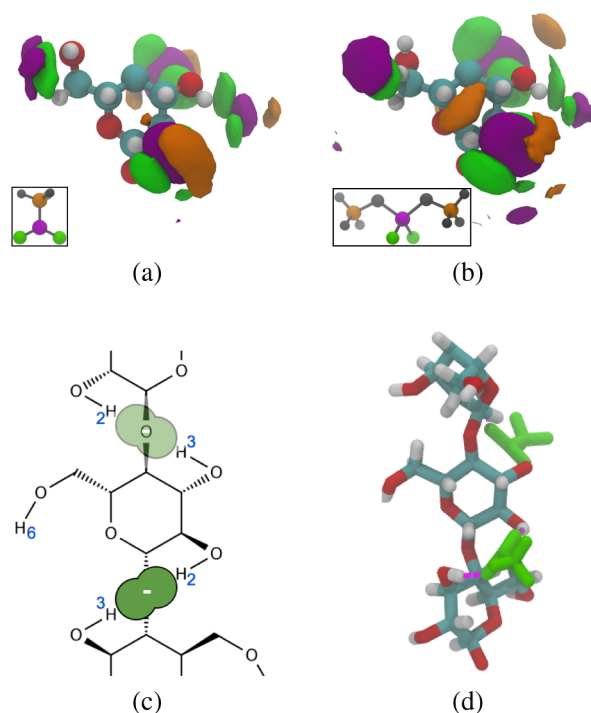


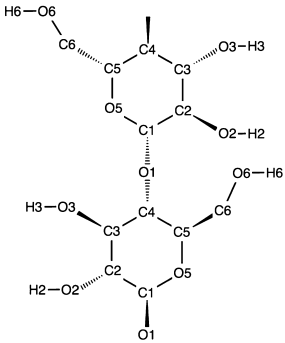
Figure 7. Spatial distribution functions for specified atoms of each anion in (a) [C₁mim]Ac and (b) [C₁mim]DMP. Isosurfaces indicate 5 times the normal density while insets provide which atoms of each anion correspond to the colored isosurfaces. (c) A depiction of the H₂–H₃ different unit anion bridge and (d) an actual snapshot showing two of these bridges simultaneously in [C₁mim]Ac.

with two consecutive bridges among three contiguous glucans. Because of the wider span of the polyatomic carboxylate and POO[−] functional groups relative to the monatomic chloride ions, the H₂ and H₃ atoms of adjacent glucans can be bridged much more readily. The formation of these bridges is significantly aided by the stereochemical structure of cellulose, with the two hydroxyl groups having orientations within the same plane of cellulose and the glycosidic bond angled away from the anion bridge.

Bridging and Nonbridging Interactions. Next, the various binding patterns between the anions and cellulose were quantified through the use of geometric criteria to determine the presence of hydrogen bonds. The occurrences of various hydrogen-bonding patterns are given for all of the ILs in Table 1. Further breakdowns of the patterns can be found in Tables S6–S8 of the Supporting Information. Overall, the acetates have the highest total number of hydrogen bonds among the three anions with approximately 3 per glucan, a 1:1 ratio of hydrogen bonds to hydroxyl groups. The chlorides have slightly less with roughly 2²/₃ per glucan while the dimethylphosphates have the least with 2¹/₃.

The details of the chart reveal that the major bridging patterns observed for the chlorides is the H_{2i}–H_{3i} pattern (Figure 6b). Because these hydroxyl groups are adjacent to one another within the same glucan, they can form two simultaneous hydrogen bonds with a single chloride with relative ease. Acetate also forms a significant number of H_{2i}–H_{3i} bridges, while dimethylphosphate forms substantially fewer, likely because of the greater steric hindrance associated with the correct positioning of the DMP anion. Both Ac and DMP also show significant numbers of the H_{2i}–H_{3j} pattern (Figure 7c), while the chloride anion has substantially fewer. As mentioned

Table 1. Occurrences of Different Hydrogen-Bonding Patterns per Glucan

	Anion	<i>n</i>	nonbridging			bridging ^a				Total ^b
			H ₆	H ₃	H ₂	H _{2i} –H _{3i}	H _{2i} –H _{6j}	H _{3i} –H _{6j}	H _{2i} –H _{3j}	
	Cl	1	0.65	0.50	0.44	0.42	0.16	0.26	0.20	2.78
		2	0.55	0.46	0.47	0.44	0.22	0.26	0.18	2.72
		3	0.56	0.24	0.39	0.72	0.24	0.20	0.12	2.60
		4	0.35	0.27	0.24	0.62	0.40	0.30	0.10	2.52
		5	0.47	0.29	0.23	0.67	0.22	0.17	0.15	2.43
	Ac	1	0.68	0.49	0.33	0.46	0.44	0.11	0.49	3.14
		2	0.63	0.31	0.22	0.58	0.37	0.14	0.56	2.80
		3	0.51	0.30	0.32	0.60	0.46	0.27	0.54	3.05
		4	0.49	0.33	0.20	0.80	0.46	0.18	0.40	3.03
		5	0.58	0.23	0.16	0.69	0.34	0.04	0.29	2.84
	DMP	1	0.52	0.33	0.25	0.25	0.22	0.12	0.58	2.34
		2	0.50	0.29	0.26	0.44	0.23	0.16	0.48	2.38
		3	0.38	0.25	0.27	0.52	0.34	0.17	0.32	2.33
		4	0.42	0.23	0.37	0.29	0.17	0.14	0.48	2.25
		5	0.44	0.30	0.26	0.32	0.12	0.16	0.30	2.29

^aIndices *i* and *j* indicate separate glucans, where *i* ≠ *j*. ^bIncludes other, less significant patterns not shown in preceding columns.

earlier, the extended range of the carboxylate and POO[−] groups relative to the chloride ions appears necessary for the formation of these patterns in significant numbers.

It was shown earlier that the concentration of anions in the first solvation shell of cellulose decreases significantly as the tail length increases, as reflected by the anion concentration in the IL bulk. Table 1 shows that despite this reduction, the hydrogen bond totals remain relatively unaffected. The reason for this is shown more clearly in Figure 8. Interestingly, as the

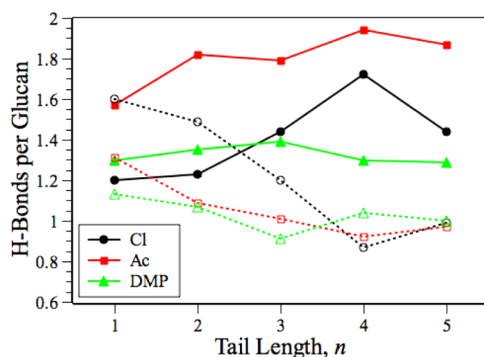


Figure 8. Effects of tail length on (dotted lines and open symbols) the hydrogen bonds produced by nonbridging anions and (solid lines and symbols) those produced from bridging anions.

tail length increases, the number of hydrogen bonds from nonbridging anions decreases while the amount of shared hydrogen bonds from bridging anions increases.

Figure 9 shows that as the number of anions in contact with cellulose decreases, there is more hydrogen bond formation per anion, minimizing the loss in overall hydrogen bond numbers. The total number of hydrogen bonds per glucan for the acetate ions drops by only 7% with increased tail length while those for the dimethylphosphate ions show almost no change (Figure 9b). The average number of hydrogen bonds formed per acetate and dimethylphosphate ion, however, increases by 14

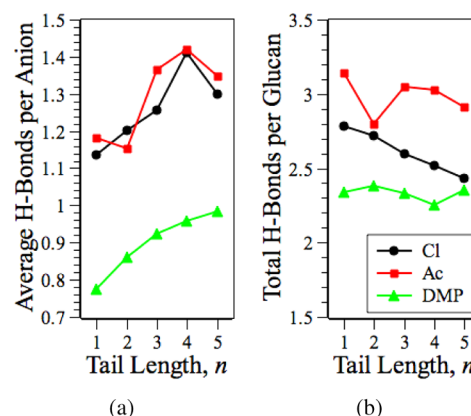


Figure 9. (a) Average number of hydrogen bonds per anion in contact with cellulose and (b) the overall average number of hydrogen bonds for the ILs.

and 27%, respectively (Figure 9a). Conversely, chloride appears more affected by this reduced anion concentration, with the overall number of hydrogen bonds per glucan dropping by 12% while the number of hydrogen bonds per anion rise by only 14%. Because of the extended reach of the Ac and DMP anions and their ability to form more bridging patterns than Cl as discussed above, it stands to reason that their character helps to moderate the loss in overall hydrogen bonds.

The Cation. Spatial Distribution Functions. We now examine how the cations organize relative to the bound anions and the cellulose chains. The SDFs showing the preferred locations of the cations were substantially weaker than for the respective anions. The trajectories of molecules in the first solvation shell revealed that the cations were considerably more mobile than their anion counterparts, likely resulting in these weaker SDFs. Nonetheless, preferred regions can certainly be identified for the imidazolium head groups; a sample SDF for [C₁mim]Cl is given in Figure 10. (This figure is representative

of the entire set, which can be found in Figures S4–S8 of the Supporting Information.)

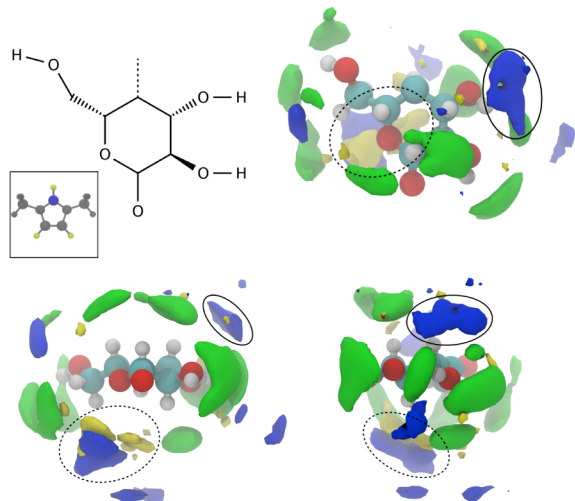


Figure 10. Spatial distribution functions showing the locations of (green) the chlorides, (blue) the C_2 atom, and (yellow) the H_1 , H_2 , and H_3 atoms of the cation in $[C_1mim]Cl$. Isosurfaces show densities that are 5 times the bulk density for the chlorides and 3 times the bulk density for the remainder. Clockwise from top left: top-down view of glucan structure, top-down view, side view, and view down the long axis of cellulose.

The isosurfaces show densities 3 times the bulk density with the C_2 carbon atom shown in blue and the ring hydrogens H_1 , H_2 , and H_3 in yellow. These are overlaid with the green chloride regions presented before, which show densities that are 5 times the bulk density. Two distinct regions of enhanced cation density can be identified and are marked by ovals in Figure 10: one between the H_{3i} – H_{6j} bridge and the nonbridged H_3 site and the other between the H_{3i} – H_{6j} bridge and the nonbridged H_2 site. Also apparent from the figures is that the former region lies near both the ether and glycosidic oxygens while the latter lies near the adjacent hydroxyl groups, both electronegative regions of the glucan.

Contacts. On the basis of the above observations, one wonders if the arrangements of the cations are dictated by the location of the bound chlorides or if they are a result of interactions with electronegative regions of cellulose. To quantify this, we calculated the number of contacts between the cation head group and any cellulose-bound anions as well as the contacts between the cation head group and the electronegative sites within cellulose. Both contact and the state of an anion being “bound” were defined as having the electronegative sites within the Lennard-Jones potential well depth, $r_m = 2^{1/6}\sigma_{ij}$, where σ_{ij} is determined via geometric mixing rules. Since these atoms experience both electronegative and van der Waals interactions, this criterion proved to be rather reliable in determining which atoms were in contact. The ring hydrogens of the cation as well as the anions were checked against all of the oxygen atoms of cellulose to determine their “boundedness” and contact. Afterwards, the ring hydrogens were again checked against the bound anions. These contact numbers were then normalized by the number of cations present in the first solvation shell; the results are given in Table 2. The results show that the ring hydrogens of the cations form roughly twice as many contacts with the bound anions than

Table 2. Number of Contacts between the Ring Hydrogens of the Cation and Cellulose-Bound Anions and Cellulose Oxygens

tail length n	number of contacts ^a					
	bound anion			cellulose		
	Cl	Ac	DMP	Cl	Ac	DMP
1	0.90	0.99	0.92	0.40	0.52	0.48
2	0.89	0.94	0.88	0.42	0.50	0.44
3	0.82	0.94	0.85	0.39	0.52	0.45
4	0.80	1.02	0.96	0.40	0.52	0.46
5	1.20	1.79	1.29	0.38	0.89	0.60

^aNormalized by the average number of cations present in the primary solvation shell of cellulose.

with cellulose, regardless of the size of the anion. The only exception to this appears to be $[C_5mim]Cl$, where there are more than 3 times as many contacts. Other studies have found comparable results for structurally similar molecules, concluding that these molecules form complexes with the anions which in turn interact with the remaining cations.^{42,43}

Combined Structure. The existence of cation–anion interactions was quite apparent from the trajectories. In fact, the first solvation shell generally consisted of large cation–anion networks, the largest of which generally constituted roughly 30% of all cations in the first solvation shell. The formation of such networks appears to be aided by the imidazolium head group being able to fit between successively bound anions on the cellulose surface, as illustrated in Figure 11. Figure 11a shows a small section of the first solvation shell of the cellulose strand. Green indicates chlorides bound to the cellulose surface, and the orange and red structures depict the cations. The three red cations are part of an alternating cation–anion chain that extends along the length of the cellulose strand. This behavior is also seen for the acetate and dimethylphosphate ILs, although the structural complexity of these anions makes it considerably more difficult to show graphically. Figure 11b shows a small network of anions and cations surrounding a small section of cellulose and again shows this cation preference for bound anions.

Though only a small subset of the solvation shell has been shown for clarity in Figure 11a,b, Figure 11c shows that these networks completely encapsulate the cellulose strand. This figure shows each connective cluster colored independently from one another and shows that the first solvation shell is largely comprised of just eight major IL clusters. We show below that the major contribution to the interaction energy from the cations arises from the van der Waals interactions; these figures, along with the SDFs of the previous sections, clearly illustrate that the polar hydroxyl groups remain occupied by the anions while the cations fill the remaining gaps between these successive sites, indirectly interacting with the nonpolar regions of cellulose.

C–H...O Hydrogen Bonds. Recently, it has been suggested, based upon NMR investigations,²³ that cations may interact directly with cellulose through the formation of weak C–H...O hydrogen bonds. To test this, the number of weak C–H...O hydrogen bonds between the cation and cellulose was calculated using a similar set of geometric criteria as before, except with an extended donor–acceptor distance of 4 Å. This criterion, used by others in the past,⁴⁴ is in agreement with the observation that C–H...O bonds extend outward to around 4

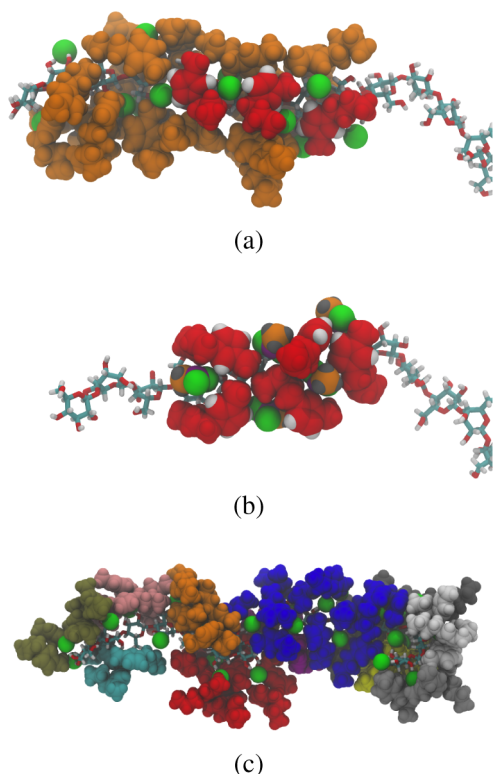


Figure 11. (a) Intercalation of $[C_4\text{mim}]$ cations (shown in red, with ring hydrogens in white) between bound chlorides (green) and (b) between bound acetates (colors corresponding to Figure 7). (c) Independent clusters formed between $[C_4\text{mim}]$ and bound chlorides. Each color represents an independent cluster taken from the contact analysis.

⁴⁵ The results of this analysis are given in Figure 12. In all cases there are substantially fewer hydrogen bonds between the

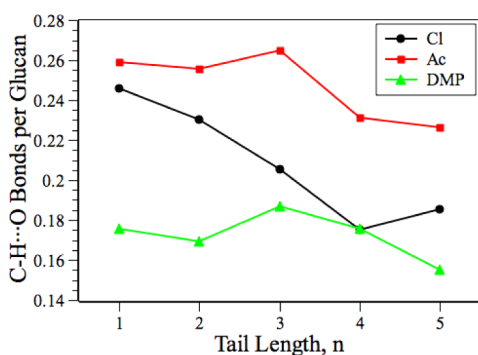


Figure 12. Occurrences of C–H...O hydrogen bonds between the imidazolium head group and the single 16-glucan cellulose strand. Standard deviations for the Cl's, Ac's, and DMP's are 0.11, 0.12, and 0.10, respectively.

cations and cellulose than between the anions and cellulose. Acetate forms the most C–H...O bonds, although its 0.25 bonds per glucan is only a fraction of the 3 hydrogen bonds per glucan formed by the anions. The chlorides form even fewer cation–cellulose hydrogen bonds, dropping from roughly 0.25 bonds per glucan to 0.2 bonds per glucan with increasing tail length while the dimethylphosphates form the fewest, with about 0.16 bonds per glucan. We note, however, that unlike the acetates and chlorides, which show a significant decrease in the

weak hydrogen bonding as a function of tail length, the dimethylphosphate ILs all form roughly the same number of weak hydrogen bonds with cellulose. These low numbers again reinforce the cation's propensity for electrostatic interaction with bound anions over direct interaction with the cellulose.

Orientation of the Alkyl Tail. The above results suggest that the head groups of the cations tend to couple with the anions at the cellulose surface. However, this leaves open the question of what happens to the alkyl tails during solvation. Clearly, their nonpolar character enables interactions with the nonpolar regions of cellulose. The orientation of the alkyl tail relative to cellulose was calculated by measuring the angle θ between the end-to-end vector of the alkyl tail and the outward normal of each glucan's cylindrical axis. A histogram of these tail orientations for the various ILs is given in Figure 13. At low tail lengths, the alkyl tails show a very mild tendency to orient away from the cellulose chain. As this length increases, however, there is a distinct shift of $\cos \theta$ toward more positive values, corresponding with an increased tendency for the tails to orient outward. This is clearly seen for the chloride series for $n = 4$ and $n = 5$ and also to a lesser extent the acetates and dimethylphosphates. These results suggest that the longer lengths force the tails to orient outward through volume exclusion effects, while nonpolar association of the tails might help stabilize this outward orientation.

Interaction Energies. Average interaction energies between the single cellulose strand and each of the different ILs were calculated using a cutoff of 12 Å. These interaction energies could be divided into contributions from the dispersion terms or the electrostatic terms and could further be attributed to either the anion or the cation. These individual contributions are listed in Table 3. Additional pairwise atom–atom energies can be found in Tables S9–S14 of the Supporting Information. Recently, it was shown that potential energy differences were a good indicator of the sign of the free energy change for $[C_4\text{mim}]\text{Cl}$,⁴⁶ allowing one to speculate on an IL's ability to dissolve crystalline cellulose. Additionally, interaction energies have been used by others to further understand the roles of the cation and the anion.^{18,22,47} The table shows that, regardless of the cation–anion pairing, the primary contribution to the attractive energy is electrostatic in nature and is derived from the anions. The contribution from the cations is significantly less, with the overall contribution being less than half that of the anion. The primary contribution from the cations derives from the van der Waals interaction and is significantly larger than their electrostatic contributions. This prevalence of the van der Waals contribution from the cation has also been noted for $[C_2\text{mim}]\text{Ac}$.⁴⁷ Here it is shown that this character extends to the other tail lengths and anions. Overall, there are only minor differences occurring in the energy contributions as a result of increasing tail length. The most noticeable of these is a diminished electrostatic attraction arising from the cations as the tail length is increased for the chlorides and the dimethylphosphates. An increased tail length could have a limiting effect on the mobility of the cation's charged head group, hindering the formation of weak C–H...O bonds with cellulose.

CONCLUSIONS

We have presented a systematic study examining the effect of the alkyl tail length on interaction energies, hydrogen bonding, and the solvation structure. Independent of the anion, we find that the tail length of the cation has only a minor influence on

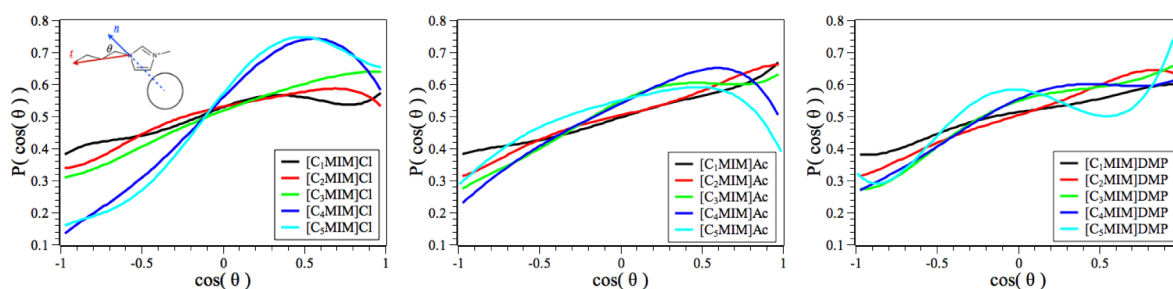


Figure 13. Orientation of the alkyl tail as a function of the tail length. Inset at left shows the vector definitions used in the calculation of θ .

Table 3. Energy Contributions, in kcal/mol, between the Different IL Components and the Cellulose Strand

anion	<i>n</i>	anion (elec)	cation (elec)	anion (vdW)	cation (vdW)	total
Cl	1	−699	99	−54	−254	−908
	2	−660	99	−60	−250	−871
	3	−628	102	−37	−254	−817
	4	−718	101	9	−248	−856
	5	−632	92	−1	−252	−793
Ac	1	−737	−124	24	−211	−1048
	2	−812	−120	33	−224	−1123
	3	−780	−134	27	−222	−1109
	4	−821	−76	39	−223	−1081
	5	−804	−94	40	−233	−1091
DMP	1	−625	−103	−80	−167	−975
	2	−685	−118	−69	−178	−1050
	3	−693	−105	−66	−181	−1045
	4	−778	−107	−56	−186	−1027
	5	−662	−76	−59	−188	−985

these quantities. Furthermore, we saw no dramatic changes in the solvation structure, hydrogen bonding, or the interaction energies of the imidazolium chlorides that would be indicative of the aforementioned “odd–even effect”. With such a dramatic influence of the tail length on dissolution, we would expect to see some indication of this in the overall interaction energies or through strong structural rearrangements. However, we find only minor fluctuations and observe very similar structures. It is possible that this effect lies rooted in the electronic structure of the ILs, requiring *ab initio* methods or the use of polarizable force fields to effectively capture this behavior. Additional experiments could also aid in understanding this peculiar behavior. We are not aware of many experimental studies outside of those existing for the imidazolium chlorides that specifically focus on these odd tail lengths. It would be very interesting to know whether or not this same odd–even behavior occurs with anions other than chloride. In a future study we plan to address this issue in a series of experiments, focusing on the other anions studied here.

Further we found that increasing or decreasing the length of the alkyl tail appears to be a simple way of controlling the bulk anion concentration. Despite these changes in the anion concentration, rearrangements in the hydrogen bonding structure ensure that losses in the overall hydrogen bonding numbers are minimal. Moreover, the solvation of cellulose and the overall interaction energy is heavily dominated by anion interactions with the polar domains of cellulose.

Cations interact directly with anions at the cellulose surface via electrostatic interactions, but they also fill the gaps between these successive sites, providing coverage of and favorable van

der Waals interactions with the nonpolar domains of cellulose. Furthermore, the dimensions of the imidazolium ring group are roughly equal to the distance between successive cellulose-bound anions, facilitating intercalation between these sites and promoting hydrophobic interactions with cellulose. The imidazolium ring, being positively charged at each end, also allows for the formation of anion–cation chains and networks at the surface of cellulose. Together, this behavior leads to strong cellulose–IL interactions without significant disruption of the IL bulk connectivity as chain length increases. It is hoped that these molecular-level insights will aid in the search for newer and better ILs for the processing of cellulose.

■ ASSOCIATED CONTENT

Supporting Information

Cation and anion SDFs for each of the ILs; detailed breakdown of pairwise energies between individual atoms; detailed breakdown of hydrogen-bonding patterns. This material is available free of charge via the Internet at <http://pubs.acs.org>.

■ AUTHOR INFORMATION

Corresponding Authors

*E-mail rabideau@ices.rwth-aachen.de; Ph +49 (0)241 8099206; Fax +49 (0)241 80628498 (B.D.R.).

*E-mail aei@alum.mit.edu; Ph +49 (0)241 8099128; Fax +49 (0)241 80628498 (A.E.I.).

Notes

The authors declare no competing financial interest.

■ ACKNOWLEDGMENTS

This work was performed as part of the Cluster of Excellence “Tailor-Made Fuels from Biomass”, which is funded by the Excellence Initiative by the German federal and state governments to promote science and research at German universities.

■ REFERENCES

- (1) Klemm, D.; Heublein, B.; Fink, H.-P.; Bohn, A. Cellulose: Fascinating Biopolymer and Sustainable Raw Material. *Angew. Chem., Int. Ed.* **2005**, *44*, 3358–3393.
- (2) Himmel, M. E.; Ding, S.-Y.; Johnson, D. K.; Adney, W. S.; Nimlos, M. R.; Brady, J. W.; Foust, T. D. Biomass Recalcitrance: Engineering Plants and Enzymes for Biofuels Production. *Science* **2007**, *315*, 804–807.
- (3) Wang, H.; Gurau, G.; Rogers, R. D. Ionic Liquid Processing of Cellulose. *Chem. Soc. Rev.* **2012**, *41*, 1519–1537.
- (4) Graenacher, C. Cellulose Solution. U.S. Patent 1,943,176, January 9, 1934.
- (5) Swatoski, R.; Spear, S.; Holbrey, J.; Rogers, R. Dissolution of Cellose with Ionic Liquids. *J. Am. Chem. Soc.* **2002**, *124*, 4974–4975.

- (6) Earle, M.; Esperanca, J.; Gilea, M.; Lopes, J.; Rebelo, L.; Magee, J.; Seddon, K.; Widegren, J. The Distillation and Volatility of Ionic Liquids. *Nature* **2006**, *439*, 831–834.
- (7) Erdmenger, T.; Haensch, C.; Hoogenboom, R.; Schubert, U. S. Homogeneous Tritylation of Cellulose in 1-Butyl-3-methylimidazolium Chloride. *Macromol. Biosci.* **2007**, *7*, 440–445.
- (8) Fukaya, Y.; Hayashi, K.; Wada, M.; Ohno, H. Cellulose Dissolution with Polar Ionic Liquids under Mild Conditions: Required Factors for Anions. *Green Chem.* **2008**, *10*, 44–46.
- (9) Vitz, J.; Erdmenger, T.; Haensch, C.; Schubert, U. S. Extended Dissolution Studies of Cellulose in Imidazolium Based Ionic Liquids. *Green Chem.* **2009**, *11*, 417–424.
- (10) Xu, A.; Wang, J.; Wang, H. Effects of Anionic Structure and Lithium Salts Addition on the Dissolution of Cellulose in 1-Butyl-3-methylimidazolium-Based Ionic Liquid Solvent Systems. *Green Chem.* **2010**, *12*, 268–275.
- (11) Zhao, H.; Baker, G.; Song, Z.; Olubajo, O.; Crittle, T.; Peters, D. Designing Enzyme-Compatible Ionic Liquids That Can Dissolve Carbohydrates. *Green Chem.* **2008**, *10*, 696–705.
- (12) Niazi, A. A.; Rabideau, B. D.; Ismail, A. E. Effects of Water Concentration on the Structural and Diffusion Properties of Imidazolium-Based Ionic Liquid-Water Mixtures. *J. Phys. Chem. B* **2013**, *117*, 1378–1388.
- (13) Mazza, M.; Catana, D.-A.; Vaca-Garcia, C.; Cecutti, C. Influence of Water on the Dissolution of Cellulose in Selected Ionic Liquids. *Cellulose* **2009**, *16*, 207–215.
- (14) Seddon, K.; Stark, A.; Torres, M. Influence of Chloride, Water, and Organic Solvents on the Physical Properties of Ionic Liquids. *Pure Appl. Chem.* **2000**, *72*, 2275–2287.
- (15) Abels, C.; Thimm, K.; Wulffhorst, H.; Spieß, A. Membrane-Based Recovery of Glucose from Enzymatic Hydrolysis of Ionic Liquid Pretreated Cellulose. *Bioresour. Technol.* **2013**, *149*, 58–64.
- (16) Brandt, A.; Hallett, J. P.; Leak, D. J.; Murphy, R. J.; Welton, T. The Effect of the Ionic Liquid Anion in the Pretreatment of Pine Wood Chips. *Green Chem.* **2010**, *12*, 672–679.
- (17) Rinaldi, R. Instantaneous Dissolution of Cellulose in Organic Electrolyte Solutions. *Chem. Commun.* **2011**, *47*, 511–513.
- (18) Zhao, Y.; Liu, X.; Wang, J.; Zhang, S. Effects of Anionic Structure on the Dissolution of Cellulose in Ionic Liquids Revealed by Molecular Simulation. *Carbohydr. Polym.* **2013**, *94*, 723–730.
- (19) Youngs, T. G. A.; Hardacre, C.; Holbrey, J. D. Glucose Solvation by the Ionic Liquid 1,3-Dimethylimidazolium Chloride: A Simulation Study. *J. Phys. Chem. B* **2007**, *111*, 13765–13774.
- (20) Youngs, T. G. A.; Holbrey, J. D.; Mullan, C. L.; Norman, S. E.; Lagunas, M. C.; D'Agostino, C.; Mantle, M. D.; Gladden, L. F.; Bowron, D. T.; Hardacre, C. Neutron Diffraction, NMR and Molecular Dynamics Study of Glucose Dissolved in the Ionic Liquid 1-Ethyl-3-methylimidazolium Acetate. *Chem. Sci.* **2011**, *2*, 1594–1605.
- (21) Rabideau, B. D.; Agarwal, A.; Ismail, A. E. Observed Mechanism for the Breakup of Small Bundles of Cellulose I-alpha and I-beta in Ionic Liquids from Molecular Dynamics Simulations. *J. Phys. Chem. B* **2013**, *117*, 3469–3479.
- (22) Zhao, Y.; Liu, X.; Wang, J.; Zhang, S. Effects of Cationic Structure on Cellulose Dissolution in Ionic Liquids: A Molecular Dynamics Study. *ChemPhysChem* **2012**, *13*, 3126–3133.
- (23) Zhang, J.; Zhang, H.; Wu, J.; Zhang, J.; He, J.; Xiang, J. NMR Spectroscopic Studies of Cellobiose Solvation in EmimAc Aimed To Understand the Dissolution Mechanism of Cellulose in Ionic Liquids. *Phys. Chem. Chem. Phys.* **2010**, *12*, 1941–1947.
- (24) Remsing, R. C.; Petrik, I. D.; Liu, Z.; Moyna, G. Comment on “NMR Spectroscopic Studies of Cellobiose Solvation in EmimAc Aimed to Understand the Dissolution Mechanism of Cellulose in Ionic Liquids” by J. Zhang, H. Zhang, J. Wu, J. Zhang, J. He, and J. Xiang. *Phys. Chem. Chem. Phys.* **2010**, *12*, 14827–14828.
- (25) Canongia Lopes, J. N.; Deschamps, J.; Padua, A. A. H. Modeling Ionic Liquids Using a Systematic All-Atom Force Field. *J. Phys. Chem. B* **2004**, *108*, 2038–2047.
- (26) Canongia Lopes, J. N.; Deschamps, J.; Padua, A. A. H. Modeling Ionic Liquids Using a Systematic All-Atom Force Field. *J. Phys. Chem. B* **2004**, *108*, 11250–11250.
- (27) Ryckaert, J.-P.; Ciccotti, G.; Berendsen, H. J. C. Numerical Integration of the Cartesian Equations of Motion of a System with Constraints: Molecular Dynamics of n-Alkanes. *J. Comput. Phys.* **1977**, *23*, 327–341.
- (28) Jorgensen, W. L.; Maxwell, D. S.; Tirado-Rives, J. Development and Testing of the OPLS All-Atom Force Field on Conformational Energetics and Properties of Organic Liquids. *J. Am. Chem. Soc.* **1996**, *118*, 11225–11236.
- (29) Banks, J.; Beard, H.; Cao, Y.; Cho, A.; Damm, W.; Farid, R.; Felts, A.; Halgren, T.; Mainz, D.; Maple, J.; et al. Integrated Modeling Program, Applied Chemical Theory (IMPACT). *J. Comput. Chem.* **2005**, *26*, 1752–1780.
- (30) Huo, F.; Liu, Z.; Wang, W. Co-Solvent or Anti-Solvent? A Molecular View on the Interface between Ionic Liquids and Cellulose when Adding Another Molecular Solvents. *J. Phys. Chem. B* **2013**, *117*, 11780–11792.
- (31) Paavilainen, S.; Róg, T.; Vattulainen, I. Analysis of Twisting of Cellulose Nanofibrils in Atomistic Molecular Dynamics Simulations. *J. Phys. Chem. B* **2011**, *115*, 3747–3755.
- (32) Matthews, J. F.; Beckham, G. T.; Bergenstrahle-Wohlert, M.; Brady, J. W.; Himmel, M. E.; Crowley, M. F. Comparison of Cellulose I Beta Simulations with Three Carbohydrate Force Fields. *J. Chem. Theory Comput.* **2012**, *8*, 735–748.
- (33) Nishiyama, Y.; Langan, P.; Chanzy, H. Crystal Structure and Hydrogen-Bonding System in Cellulose I Beta from Synchrotron X-ray and Neutron Fiber Diffraction. *J. Am. Chem. Soc.* **2002**, *124*, 9074–9082.
- (34) Hockney, R. W.; Eastwood, J. W. *Computer Simulation Using Particles*; Adam Hilger-IOP: Bristol, UK, 1988.
- (35) Plimpton, S. Fast Parallel Algorithms for Short-Range Molecular-Dynamics. *J. Comput. Phys.* **1995**, *117*, 1–19.
- (36) Chandra, A. Effects of Ion Atmosphere on Hydrogen-Bond Dynamics in Aqueous Electrolyte Solutions. *Phys. Rev. Lett.* **2000**, *85*, 768–771.
- (37) Chowdhuri, S.; Chandra, A. Hydrogen Bonds in Aqueous Electrolyte Solutions: Statistics and Dynamics Based on Both Geometric and Energetic Criteria. *Phys. Rev. E* **2002**, *66*, 041203.
- (38) Luzar, A.; Chandler, D. Structure and Hydrogen-Bond Dynamics of Water-Dimethyl Sulfoxide Mixtures by Computer-Simulations. *J. Chem. Phys.* **1993**, *98*, 8160–8173.
- (39) Luzar, A.; Chandler, D. Effect of Environment on Hydrogen Bond Dynamics in Liquid Water. *Phys. Rev. Lett.* **1996**, *76*, 928–931.
- (40) Luzar, A.; Chandler, D. Hydrogen-Bond Kinetics in Liquid Water. *Nature* **1996**, *379*, 55–57.
- (41) Luzar, A. Resolving the Hydrogen Bond Dynamics Conundrum. *J. Chem. Phys.* **2000**, *113*, 10663–10675.
- (42) Hanke, C.; Atamas, N.; Lynden-Bell, R. Solvation of Small Molecules in Imidazolium Ionic Liquids: a Simulation Study. *Green Chem.* **2002**, *4*, 107–111.
- (43) Rabideau, B. D.; Ismail, A. E. The Effects of Chloride Binding on the Behavior of Cellulose-Derived Solutes in the Ionic Liquid 1-Butyl-3-methylimidazolium Chloride. *J. Phys. Chem. B* **2012**, *116*, 9732–9743.
- (44) Liu, H.; Sale, K.; Simmons, B.; Singh, S. Molecular Dynamics Study of Polysaccharides in Binary Solvent Mixtures of an Ionic Liquid and Water. *J. Phys. Chem. B* **2011**, *115*, 10251–10258.
- (45) Koch, U.; Popelier, P. L. A. Characterization Of C–H–O Hydrogen-Bonds on the Basis of the Charge-Density. *J. Phys. Chem.* **1995**, *99*, 9747–9754.
- (46) Gross, A. S.; Bell, A. T.; Chu, J.-W. Entropy of Cellulose Dissolution in Water and in the Ionic Liquid 1-Butyl-3-methylimidazolium Chloride. *Phys. Chem. Chem. Phys.* **2012**, *14*, 8425–8430.
- (47) Liu, H.; Sale, K. L.; Holmes, B. M.; Simmons, B. A.; Singh, S. Understanding the Interactions of Cellulose with Ionic Liquids: A Molecular Dynamics Study. *J. Phys. Chem. B* **2010**, *114*, 4293–4301.